Scanning Microscopy

Volume 1992
Number 6 *Signal and Image Processing in Microscopy and Microanalysis*

Article 8

1992

Measurement of Electron-Optical Parameters for High-Resolution Electron Microscopy Image Interpretation

A. F. de Jong
Philips Electron Optics, The Netherlands

A. J. Koster
Tietz Video and Image Processing Systems GmbH, Germany

Scanning Microscopy Supplement 6, 1992 (pages 95-103) 0892-953X/92$5.00+.00
Scanning Microscopy International, Chicago (AMF O'Hare), IL 60666 USA

MEASUREMENT OF ELECTRON-OPTICAL PARAMETERS FOR HIGH-RESOLUTION ELECTRON MICROSCOPY IMAGE INTERPRETATION

A.F. de Jong* and A.J. Koster[1,2]

Philips Electron Optics, AAE-p, P.O.Box 218, 5600 MD Eindhoven, The Netherlands
[1]Tietz Video and Image Processing Systems GmbH, Herbststrasse 7, D-82131 Gauting, Germany
[2]Present address: Max-Plack Inst. Biochem., Dept. Structural Biology, D-82152 Martinsried, Germany

Abstract

A method is presented to measure various electron-optical parameters needed for high-resolution electron microscopy image interpretation with high accuracy. The method is based on the measurement of a series of beam-tilt induced image displacements. The displacements are calculated via cross-correlation of the images, and subsequently fitted to a third-order polynomal in the beam tilt. From two series of images (using the x and y beam tilt coils), the spherical aberration constant of the microscope can be measured, as well as the current values of defocus, beam tilt and astigmatism. The spherical aberration constant of three Philips microscopes is measured with a precision better than 1%, apart from calibration errors.The misalignment in the reference image (i.e. without *induced* beam tilt) can be measured with an absolute accuracy of 0.05 mrad, while the accuracy in the measured defocus value is 5 nm (at a magnification of 250,000). A computer is used to direct the experiments via remote control of the microscope and perform fast image processing to calculate the cross-correlations.

Key Words: Transmission electron microscopy, high resolution electron microscopy, electron optics, contrast transfer function, induced beam tilts, image shifts, computer control, image processing, spherical aberration coefficient

*Address for correspondence:
A. Frank de Jong
Philips Electron Optics, AAE-p
P.O. Box 218
5600 MD Eindhoven
The Netherlands
Telephone number: 31-40-766084
FAX number: 31-40-766820

Introduction

The measurement of electron-optical parameters in the transmission electron microscope (TEM) is important for two reasons. In the first place, fast and accurate measurement of parameters like focus, astigmatism and beam tilt enables the automatic *correction* of astigmatism and misalignment (referred to as autotuning). In the second place, several electron-optical parameters must be *known* to a high accuracy in order to be able to interprete high-resolution TEM (HREM) images, using either image simulation or image reconstruction (via a focal series or via holography). The incorporation of the aberrations of the microscope via the contrast transfer function is then an important step. Especially when the interpretation aims at resolving features at a resolution beyond the Scherzer limit, the accuracy with which the phase part of the transfer function must be known increases dramatically.

The aim of *autotuning* is to be an aid to the microscope operator. Hence, the autotuning procedures must be as accurate as an experienced operator, and significantly faster. Furthermore, a good autotuning procedure must be fully automated and must be designed as robust as possible to give reliable results for a wide range of (unknown) experimental conditions. On the other hand, procedures which aim at *measuring* electron-optical parameters must be very accurate, but the requirements on speed, automation and robustness are not as heavy as for the autotuning procedure. Hence, procedures aimed at accurate measurement for HREM image interpretation may be somewhat more complicated, if necessary.

For TEM autotuning, several methods have been proposed (see Erasmus and Smith, 1982 and Smith et al., 1983 for an overview). The methods proposed use either image contrast, or diffractograms, or beam-tilt induced image displacements. The image contrast method uses the fact that the image contrast in the TEM is minimal in a focussed image without astigmatism (Saxton et al., 1983). The method iterates to the zero-values of focus and astigmatism using induced variations of these parameters. The digital diffractogram (powerspectrum) of an amorphous image yields the (square of the) phase transfer function of the microscope. It can be calculated very fast and a quasi-continuous display of the diffractogram is more and more frequently used as an aid for manual alignment. An on-line alignment algorithm for the correction of astigmatism has been implemented by Baba et al. (1987). However, the effects of misalignment and astigmatism cannot be distinguished in one diffractogram and several diffractograms with an induced beam tilt (in various azimuths) must be used to measure both astigmatism and misalignment (Zemlin et al. 1978). Although it is nowadays possible to display such a "plateau" of diffractograms on-line (de Ruyter

et al. 1990), this method is not very robust. The shape of the diffractograms (with induced beam tilts) may vary strongly with the initial experimental conditions (focus, misalignment, astigmatism and sample type), hampering automatic evaluation. The most promising method for autotuning seems to be the measurement of beam-tilt induced image shifts, as proposed by Koster et al. (1987) and Koster (1988). The basic idea (LePoole, 1947) is that when the image is out of focus, an induced beam tilt results in an image shift. The image shifts can nowadays be determined very accurately using fast cross-correlation of the images. Incorporation of astigmatism is straight-forward, while the measurement of the misalignment requires the *difference* of the shifts of two images with opposite induced beam tilt. Practical implementation of the method and results are reported by Koster and de Ruyter (1992).

However, the demands on the accuracy of the electron-optical parameters to be used for image reconstruction are very high. Several promising methods are currently being developed which are in principle able to yield reconstructed images with a resolution far beyond the point resolution of the microscope: electron holography (see e.g. Lichte, 1986), and image reconstruction using a focal series (Kirkland, 1984, Van Dyck and Op de Beeck, 1990). Recent progress in these methods is reported by Lichte (1991a) and Van Dyck (1991). All the reconstruction methods first solve the phase problem, yielding the electron wavefunction in the image plane. As a second step, this wavefunction is multiplied by the inverse contrast transfer function, yielding the electron wavefunction in the object plane, corrected for aberrations. Especially at higher resolutions, the contrast transfer function oscillates strongly with spatial frequency. Its exact shape must be known to a high accuracy, or large errors in the phase will be introduced during the final step of the reconstruction. Of the parameters determining the phase contrast transfer function (PCTF), the constant of sperical aberration C_s is the most critical one. Kirkland and Siegel (1979) found that a maximum error of less than 5% in C_s is required to be able to recover information from electron micrographs below the point-resolution. Note that it is not possible to determine the parameters of the phase transfer function during the reconstruction process, unless some a-priori knowledge is used about the object (e.g. the crystal symmetry). Even then, it will be advantageous or even necessary to start with an accurate set of values for C_s, defocus and residual astigmatism and misalignment.

In this paper, the accuracy of the electron-optical parameters required for image reconstruction is calculated as a function of the desired resolution. A method is proposed and tested which determines the spherical aberration coefficient of the microscope very accurately, as well as the defocus value and residual misalignment and astigmatism. The method uses beam-tilt induced image shifts, but it is somewhat more complex than the related autotuning method (see also Budinger and Glaeser, 1976 and Koster and de Jong, 1991). It can be used to measure the parameters needed for image reconstruction, but also to check existing autotuning procedures independently and assess their quality. The spherical aberration coefficients of three microscopes (Philips CM12-TWIN, CM20-UltraTWIN and CM30-SuperTWIN) are measured with a precision better than 1%, and the accuracy with which the values of defocus and residual beam tilt and astigmatism can be measured is assessed. Of the other two methods used for autotuning, the image contrast method is not suitable for a measuring procedure. However, the method of using several diffractograms could be an alternative, because use can now be made of the known, approximate values of the PCTF parameters to generate the type of patterns which can be more easily analysed in the computer.

Theory

Required accuracy of the parameters of the PCTF

It is well known that the image contrast in HREM is strongly influenced by the contrast transfer of the microscope. Within the quasi-coherent approximation (Wade and Frank, 1977), the relation (in reciprocal space) between the (aberrated) wavefunction in the image plane, $\Psi_{ima}(\boldsymbol{G})$ and the wavefunction at the exit plane of the object, $\Psi_{obj}(\boldsymbol{G})$ is a simple product with a transfer function $\Gamma(\boldsymbol{G})$:

$$\Psi_{ima}(\boldsymbol{G}) = \Gamma(\boldsymbol{G})\Psi_{obj}(\boldsymbol{G}). \tag{1}$$

Here, $\boldsymbol{G}$ is a two-dimensional vector in reciprocal space with a length $G=1/R$. For unit magnification and no image rotation we have:

$$\Gamma(\boldsymbol{G}) = E(\boldsymbol{G})\exp[-2\pi i\chi(\boldsymbol{G})]. \tag{2}$$

The phase-contrast transfer function, $\exp[-2\pi i\chi(\boldsymbol{G})]$, is the part of the transfer function which oscillates strongly at higher spatial frequencies. Including a beam tilt $\boldsymbol{m}$ (misalignment) and an astigmatism $A\boldsymbol{a}$, it is given by:

$$\begin{aligned}\chi(\boldsymbol{G}) &= \tfrac{1}{4}C_s\lambda^3(\boldsymbol{G}+\boldsymbol{m})^4 + \tfrac{1}{2}\lambda\left(f - \tfrac{1}{2}A\right)(\boldsymbol{G}+\boldsymbol{m})^2 + \\ &\quad \tfrac{1}{2}\lambda A((\boldsymbol{G}+\boldsymbol{m})\bullet\boldsymbol{a})^2 \\ &= \tfrac{1}{4}C_4(\boldsymbol{G}+\boldsymbol{m})^4 + \tfrac{1}{2}C_2(\boldsymbol{G}+\boldsymbol{m})^2 + \\ &\quad \tfrac{1}{2}C_A((\boldsymbol{G}+\boldsymbol{m})\bullet\boldsymbol{a})^2,\end{aligned} \tag{3}$$

where f is the defocus (negative for underfocus) and λ the electron wavelength. In eq. (3), we have defined the constants C_4, C_2 and C_A as the parameters which, together with the beam tilt $\boldsymbol{m}$, and the direction of the astigmatism $\boldsymbol{a}$, (in total six independent parameters) have to be known in order to reconstruct the PCTF. Note that the wavelength as such does not have to be known. The envelope function $E(\boldsymbol{G})$ is determined by the finite beam convergence and by the focus spread due to the chromatic aberration and microscope instabilities. It attenuates the amplitude of Γ, limiting the final resolution of the instrument (information limit). Its exact form can be found elsewhere (e.g. Frank, 1973 and Wade and Frank, 1977), but will not be considered here.

Errors in the PCTF are caused by errors in the determination of the C_s, defocus, astigmatism, beam-tilt misalignment and magnification (i.e. an error in $\boldsymbol{G}$). The wavelength as such is in fact only a scaling parameter and not a source of error, as long as the accelerating voltage of the microscope is reasonably stable. Note that the misalignment and astigmatism do not have to be zero, as long as they are known (and not too large to degrade the image quality). To illustrate the importance of an accurate determination of C_s, we have calculated the imaginary part of the transfer function of a 200 kV microscope with Field-emission gun (FEG) in Fig. 1. Because of the high spatial and temporal coherence caused by the FEG, there is a lot of contrast-transfer beyond the point resolution of the microscope. However, the PCTF oscillates with increasing spatial frequency. When the PCTF is calculated with a C_s of only 2% more, the oscillations at higher frequencies are even reversed in sign. On the other hand, close

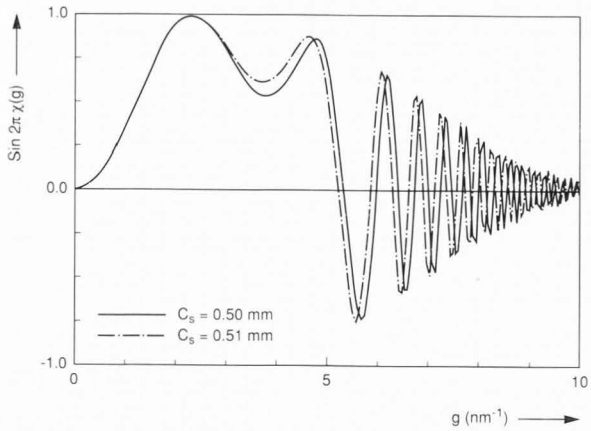

Fig. 1. Imaginary part of the contrast transfer function $\Gamma(G)$ for a 200 kV microscope with a FEG, at Scherzer focus.

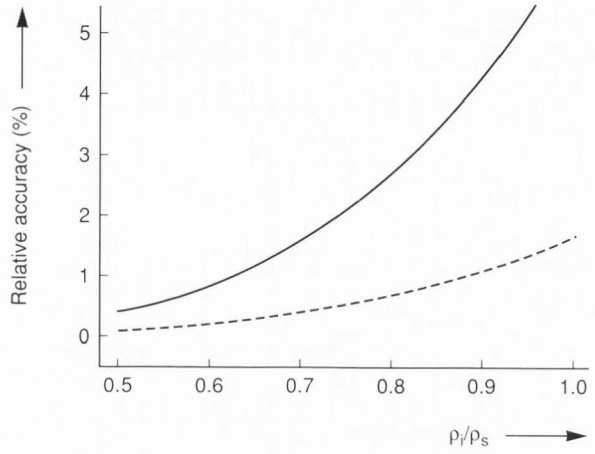

Fig. 2. Maximum allowable relative accuracy in C_s and magnification, as a function of the ratio between information limit and point resolution. Solid curve: accuracy in the C_s, and magnification in the case of optimum focus. Dashed: accuracy for the magnification in the case of Gaussian focus. The curves can also be used to determine the (absolute) allowable accuracy for the beam tilt, by dividing the values for the magnification by ρ_i.

---

to the point resolution the effect is only small. This indicates that higher accuracies are needed when the information retrieval is aimed at higher resolutions (relative to the point resolution of the microscope). Following Kirkland and Siegel (1979), we will assume that the maximum total error in the phase may not exceed $\pi/3$, for the range of frequencies involved. Neglecting for the moment the astigmatism (which is just a directional focus-error), we find:

$$2\pi\,\Delta\,\chi(\boldsymbol{G}) =$$

$$2\pi\sqrt{(\Delta\,\chi_{Cs})^2+(\Delta\,\chi_f)^2+(\Delta\,\chi_m)^2+(\Delta\,\chi_G)^2} \le \tfrac{1}{3}\pi. \tag{4}$$

Each individual error, which may be found by making a Taylor series expansion, must be below $\pi/6$. Thus criteria for the individual errors may be easily derived. We will formulate the maximum allowable errors in terms of the point resolution of the microscope, defined as $\rho_s=0.64(C_s\lambda^3)^{0.25}$ and of the desired information limit ρ_i (which is the inverse of the maximum spatial frequency). Because χ is linearly dependent on C_s and f, their maximum allowable errors are simply given by:

$$\frac{\Delta C_s}{C_s} = \frac{1}{3}\left(\frac{2\,\rho_i}{3\,\rho_s}\right)^4, \tag{5}$$

$$\Delta f = \frac{\rho_i^2}{6\,\lambda}. \tag{6}$$

In Fig. 2, the maximum error in C_s is given as a function of the ratio between ρ_i and ρ_s. The influence of errors in the misalignment and the magnification is dependent on the amount of defocus. Assuming that the microscope is well aligned, so that $m<<G$, we find for the maximum allowable error in magnification:

$$\frac{\Delta G}{G} = \frac{1}{12}\left[\left(\frac{3\,\rho_s}{2\,\rho_i}\right)^4 + \frac{C_2}{\rho_i^2}\right]^{-1}. \tag{7}$$

Clearly the maximum error is rather small for defocus values around Gaussian focus, while there is a singularity where at $G=1/\rho_i$ the focus part just compensates the C_s part in the denominator. However, when this focus value is chosen, the error due to ΔG is high at some intermediate frequency. To get a practical idea of the maximum allowable error, we will choose as a reasonable defocus value the "optimal" focus. At the optimal focus the error due to errors in misalignment and magnification is minimal for the whole range of spatial frequencies between 0 and $G=1/\rho_i$. This value can be found by requesting that the maximum value of $|\partial\chi(\boldsymbol{G})/\partial\boldsymbol{G}|$ is minimized. The optimal focus, which also maximizes the image localization during imaging with a highly coherent probe (Lichte, 1991b), is then found as $f_{opt} = -0.75C_s(\lambda/\rho_i)^2$. Substituting the values for Gaussian focus and optimal focus into eq. (7) yields:

$$\left(\frac{\Delta G}{G}\right)_{opt} = \frac{1}{3}\left(\frac{2\,\rho_i}{3\,\rho_s}\right)^4,$$

$$\left(\frac{\Delta G}{G}\right)_{Gauss} = \frac{1}{12}\left(\frac{2\,\rho_i}{3\,\rho_s}\right)^4. \tag{8}$$

This error is also illustrated in Fig. 2, for the two defocus values. In practical situations the allowable error will lay between these two curves. The maximum allowable error in the determined misalignment, given in absolute units of (length)$^{-1}$, is:

$$(\Delta\,m)_{opt} = \frac{1}{3\,\rho_i}\left(\frac{2\,\rho_i}{3\,\rho_s}\right)^4,$$

$$(\Delta\,m)_{Gauss} = \frac{1}{12\,\rho_i}\left(\frac{2\,\rho_i}{3\,\rho_s}\right)^4. \tag{9}$$

Table 1. Some typical values of the accuracy needed in the determination of the parameters of the PCTF to ensure a reconstruction of the PCTF with an error below $\pi/3$ for the desired range of spatial frequencies (H.T. is high tension).

H.T. (kV)	ρ_s (nm)	ρ_i (nm)	ΔC_s (%)	Δf (nm)	Δm (mrad)	ΔG (%)
200	0.24	0.15	0.8	1.5	0.04-0.14	0.2-0.8
		0.10	0.2	0.7	0.01-0.04	0.05-0.2
200	0.19	0.15	2.2	1.5	0.10-0.4	0.5-2.2
		0.10	0.4	0.7	0.03-0.11	0.1-0.4
300	0.17	0.15	3.4	2.0	0.10-0.4	0.85-3.4
		0.10	0.7	0.8	0.03-0.12	0.15-0.7

A number of maximum errors of practical importance (200-300 keV beam energy, C_s from 0.5 to 1.2 mm) are given in Table 1. If an ultimate resolution around 0.1 nm is to be reached, even with ultra-high-resolution pole-pieces the allowable errors are extremely small, roughly around 0.5% for the C_s and the magnification, 1 nm for defocus and 0.05 mrad for the misalignment. Note that the accuracy needed for the defocus is less than the specimen thicknesses normally used for HREM. Trying to determine the defocus value to this accuracy is rather academic, as it is not clear to which depth inside the specimen this focus refers.The accuracy needed for the determination of the astigmatism can easily be calculated to be twice the allowable error for the defocus, i.e. about 2 nm for ρ_i=0.1 nm.

An effect which has not yet been taken into account is the asymmetric energy spread of the electron gun. Through this effect, the time-averaging of a small amount of focus values in one exposure (focal spread function) is asymmetric, which could lead to an additional phase term in the contrast transfer function. An estimate about the implications of the asymmetry can be made as follows. Suppose we have an effective asymmetry in the energy spread of 1 ppm (i.e. 0.3V for 300 kV accelerating voltage). Then also the asymmetry in the focal spread is 1 ppm (related to the focal length of the objective lens), which could have the same effect as an uncertainty in the defocus value of 1 to 2 nm.

Beam-tilt induced image shift

From a geometrical point of view, it is not difficult to understand that at low magnification the primary result of applying a beam tilt is an image displacement. In Fig. 3, it is illustrated that the displacement has two components: a first displacement caused by a possible focus error and a second displacement caused by the spherical aberration of the objective lens. Budinger and Glaeser (1976) gave a theoretical description for this displacement (for lower magnifications under two-beam conditions) and described a method to determine the C_s and the defocus by measuring the displacement between a bright-field and two centered dark-field images with different scattering vectors. The description given in this paper is based on HREM imaging theory in weak phase-object approximation (see also Koster et al., 1989), which is suitable for HREM situations when an amorphous (part of the) specimen is used for the measurements.

Within the weak phase-object approximation, the complex image spectrum $I(\boldsymbol{G})$ (i.e. the Fourier transform of the image) can be written as:

$$I(\boldsymbol{G}) = \delta(\boldsymbol{G}) - 2\sigma V(\boldsymbol{G})E(\boldsymbol{G})\sin[2\pi\chi_e(\boldsymbol{G})]\exp[-2\pi i\chi_o(\boldsymbol{G})]. \tag{10}$$

Here $V(\boldsymbol{G})$ is the elastic scattering potential of the specimen, $\sigma=\pi e/\lambda E$ and the phase-transfer function is divided into two parts, even and uneven in $\boldsymbol{G}$:

$$\chi_e(\boldsymbol{G}) = \tfrac{1}{4}C_4\{G^4 + 4(\boldsymbol{G}\bullet\boldsymbol{K})^2 + 2G^2K^2\} + \tfrac{1}{2}C_2G^2 + \tfrac{1}{2}C_A((\boldsymbol{G}+\boldsymbol{K})\bullet\boldsymbol{a})^2, \tag{11a}$$

$$\chi_o(\boldsymbol{G}) = \{C_4(G^2+K^2) + C_2\}(\boldsymbol{G}\bullet\boldsymbol{K}) + C_A(\boldsymbol{G}\bullet\boldsymbol{a})(\boldsymbol{K}\bullet\boldsymbol{a}), \tag{11b}$$

for a beam tilt $\boldsymbol{K}$. If we now consider two images with a different beam tilt $\boldsymbol{K}_1$ and $\boldsymbol{K}_2$, the cross-spectrum of the two (which is the Fourier transform of the cross-correlation function) is:

$$I_1(\boldsymbol{K}_1)I_2^*(\boldsymbol{K}_2) = \delta + 4\sigma^2V^2E(\boldsymbol{K}_1)E(\boldsymbol{K}_2)\times \sin[2\pi\chi_e(\boldsymbol{K}_1)]\sin[2\pi\chi_e(\boldsymbol{K}_2)]\times \exp[2\pi i\{\chi_o(\boldsymbol{K}_2) - \chi_o(\boldsymbol{K}_1)\}], \tag{12}$$

where we have stressed the dependence on beam tilt rather than on the spatial frequency. When the beam tilts involved are not too high, the envelope function $E(\boldsymbol{G},\boldsymbol{K})$ and the even part of the phase-transfer function $\chi_e(\boldsymbol{G},\boldsymbol{K})$ may be considered to be independent of $\boldsymbol{K}$ (double-sideband imaging). In that case, the cross-spectrum may be approximated by:

$$I_1(\boldsymbol{K}_1)I_2^*(\boldsymbol{K}_2) \cong \delta + A(\boldsymbol{G})\exp[2\pi i\{\chi_o(\boldsymbol{K}_2) - \chi_o(\boldsymbol{K}_1)\}]. \tag{13}$$

The amplitude function $A(\boldsymbol{G})$ is now independent of the beam tilt. The phase of the cross-spectrum is linearly dependent on $\boldsymbol{G}$ (eq. (11b)), apart from the term $C_4G^2\boldsymbol{G}.(\boldsymbol{K}_2-\boldsymbol{K}_1)$, which results in a dispersion for the higher spatial frequencies. If this term can be neglected in comparison to e.g. the focus term (which may easily be obtained by applying a low-pass filter) the inverse Fourier transform of eq. (13) yields the cross-correlation function between the two images:

$$c(\boldsymbol{R}) = 1 + a(\boldsymbol{R}) * \delta(\boldsymbol{R} - \boldsymbol{d}). \tag{14}$$

Here $a(\boldsymbol{R})$, the inverse Fourier transform of $A(\boldsymbol{G})$, is just the auto-correlation function of the image itself. The convolution with a delta-function indicates that this sharply peaked function is displaced over a vector $\boldsymbol{d}$, given by the derivative of the odd parts of the phase transfer function with respect to $\boldsymbol{G}$. For the case that image 1 has only a misalignment $\boldsymbol{m}$, while image 2 has an additional induced beam tilt $\boldsymbol{t}$, the displacement is given by:

$$\boldsymbol{d} = C_4\{(\boldsymbol{t}+\boldsymbol{m})^3 - \boldsymbol{m}^3\} + C_2\boldsymbol{t} + C_A(\boldsymbol{t}\bullet\boldsymbol{a})\boldsymbol{a}. \tag{15}$$

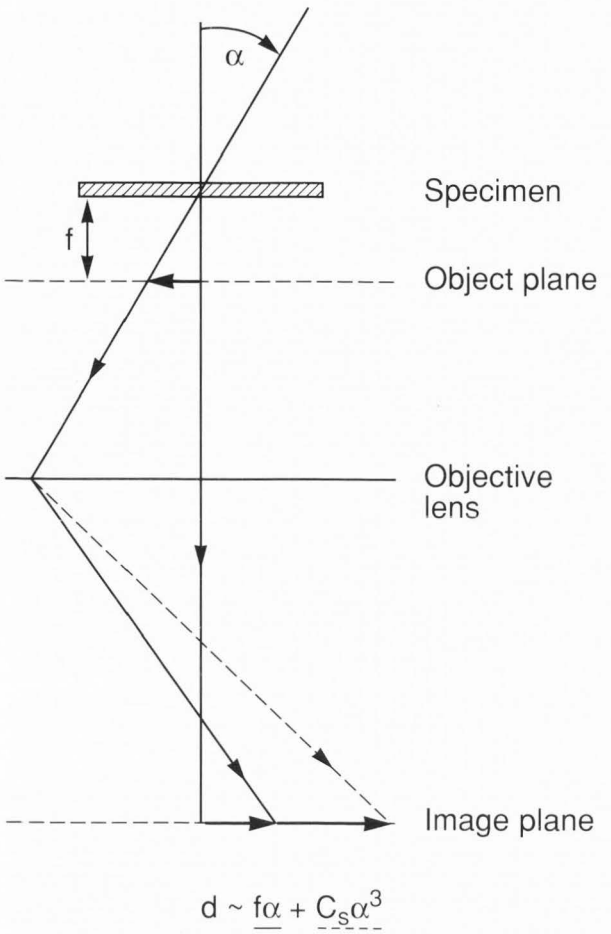

Fig. 3. Schematic presentation of the image displacement caused by an induced beam tilt angle α. The focus error f induces a displacement proportional to the angle, the spherical aberration adds a displacement proportional to the third power of the angle.

For autotuning purposes, the induced beam tilts applied are usually well within the limits of double sideband imaging, so that the approximation of the cross-correlation as yielding a shifted sharp peak is justified. However, for the more accurate measurements proposed here, the range of induced tilts may reach beyond this region. The amplitude parts in eq. (12) are then no longer independent of the beam tilt, but give rise to contrast reversals, so that the position of a (local) minimum instead of a maximum has to be determined. Still, the cross-correlation function can be considered to be a more or less peaked feature (positive or negative), displaced by $\boldsymbol{d}$. Although in this section the influence of an induced beam tilt is described within the framework of a weak phase-object, it may be appreciated that a small amplitude component in the contrast will not immediately degrade the method, because to a first approximation, only the autocorrelation of the image is affected. This approximation of course breaks down for thicker (crystalline) specimens where the induced tilt affects the dynamical scattering within the sample.

Measuring PCTF parameters

The displacement is a third-order polynomial of the beam tilt and all the parameters of the PCTF may be determined by measuring a series of image displacements as a function of the beam tilt $\boldsymbol{t}$. However, inspection of eq. (15) reveals that the total displacement is in fact a sum of contributions in three directions: along $\boldsymbol{t}$, $\boldsymbol{m}$ and $\boldsymbol{a}$. Thus, also the direction of the measured displacement is dependent on the induced tilt. An induced tilt in the x beam tilt coil will in general result in a displacement d_{xx} parallel to the x-direction and a displacement d_{xy} perpendicular to this direction (in the axis system determined by the beam tilt coils). When a series of beam tilts is applied, the image displacement follows a trajectory as illustrated by some simulated trajectories in Fig. 4. The presence of astigmatism and/or misalignment causes only a small (but measurable) deviation from the parallel direction. At higher induced beam tilts, the third-order contribution in the direction of the induced tilt dominates the displacement.

Eq. (15) can be rewritten as follows, with α,β signifying the x or y direction in the axis system of the beam tilt coils:

$$d_{\alpha\beta} = \sum_n \Theta_{n\alpha\beta} (t_\alpha)^n, \tag{16}$$

with

$$\Theta_{3\alpha\alpha} = C_4, \tag{17a}$$

$$\Theta_{2\alpha\alpha} = 3C_4 m_\alpha, \tag{17b}$$

$$\Theta_{1\alpha\alpha} = C_4\left(3m_\alpha^2 + m_\beta^2\right) + C_2 + C_A a_{\alpha}^2 \tag{17c}$$

$$\Theta_{3\alpha\beta} = 0, \tag{17d}$$

$$\Theta_{2\alpha\beta} = C_4 m_\beta, \tag{17e}$$

$$\Theta_{1\alpha\beta} = 2C_4 m_\alpha m_\beta + C_A a_\alpha a_\beta. \tag{17f}$$

Note that $\Theta_{1\alpha\beta} = \Theta_{1\beta\alpha}$ and $\Theta_{3\alpha\alpha} = \Theta_{3\beta\beta}$. The displacements at high induced tilts may be used to determine the (apparent) rotation of the axis system of the beam tilt coils with respect to the axis system of the image (determined by the image detector)

By measuring a series of displacements as a function of the induced beam tilt, several parameters may be found by fitting the parallel displacements to a third-order curve and the perpendicular displacements to a second order curve. From one series of parallel displacements (three coefficients fitted) one may find C_4 (from $\Theta_{3\alpha\alpha}$) and the misalignment in the direction of the induced tilt (from $\Theta_{2\alpha\alpha}$). The first-order coefficient (from $\Theta_{1\alpha\alpha}$) does only yield C_2 value in a straightforward manner, when both the misalignment and the astigmatism are zero. When, in addition, the perpendicular displacements are used (two fitted coefficients), the misalignment perpendicular to the induced tilt may be found (from $\Theta_{2\alpha\beta}$). However, the five coefficients which may be fitted from one series of diplacements are not enough to determine the six parameters needed for the reconstruction of the PCTF. Specifically, knowledge of $\Theta_{1\alpha\alpha}$ and $\Theta_{1\alpha\beta}$ is not enough to determine C_2, C_A and the ratio a_x/a_y. Moreover, the determination of the two perpendicular coefficients is usually less accurate than the parallel coefficients. To obtain all six parameters with high accuracy, it is necessary to measure one tilt series along x and one along y. The constant C_4 may be found from $\Theta_{3\alpha\alpha}$ and $\Theta_{3\beta\beta}$, the misalignments from $\Theta_{2\alpha\alpha}$ and $\Theta_{2\beta\beta}$. The defocus value λf may be found by adding $\Theta_{1\alpha\alpha}$ and $\Theta_{1\beta\beta}$, from eq. (17c) and using $a_x^2 + a_y^2 = 1$:

$$\lambda f = \tfrac{1}{2}\left(\Theta_{1\alpha\alpha} + \Theta_{1\beta\beta}\right) - \frac{2}{9\Theta_{3\alpha\alpha}}\left(\Theta_{2\alpha\alpha}^2 + \Theta_{2\beta\beta}^2\right) \tag{18}$$

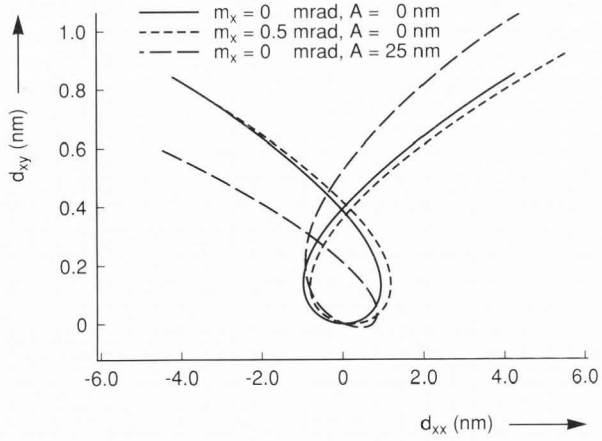

Fig. 4. Simulated trajectories of the image displacement $\boldsymbol{d}$ caused by an induced beam tilt along the x-direction. For all the curves, the accelerating voltage is 300 kV, C_s= 1.2 mm, f = -200 nm and the misalignment in the y-direction, m_y = 1.0 mrad. Note the difference in scale along the vertical and horizontal axes.

The astigmatism is then finally found from the four first-order coefficients.

If we include the magnification M and the tilt increment d$\boldsymbol{t}$ into eq. (16), we obtain the polynomials which are actually fitted in a real experiment:

$$\boldsymbol{d'}_{\alpha\beta} = M \sum_n \Theta_{n\alpha\beta} (\mathrm{d}\, t_\alpha\, t'_\alpha)^n. \qquad (19)$$

Then the shift is measured in pixels and the beam tilt in "ticks", being the smallest unit-of-change of the beam-tilt coils. Clearly, both the magnification and the induced beam tilt must be calibrated accurately in order to determine the PCTF parameters. Especially C_4, calculated from the third-order coefficient, is sensitive to calibration errors of the beam tilt. The beam tilt may be calibrated by measuring the displacement of the diffraction pattern, relative to the diffraction vector $\boldsymbol{G}$ corresponding to some known lattice distance d_{hkl}. If a relative distance of r is measured in the diffraction plane, the beam tilt $\boldsymbol{t}$ causing this displacement is r/d_{hkl} (in units of (length)$^{-1}$). As the beam tilt calibration may be (slightly) different for the x and the y direction, both beam tilts should be calibrated. Also a slight deviation from orthogonality may be taken into account. The difference between the two fitted third-order coefficients $\Theta_{3\alpha\alpha}$ and $\Theta_{3\beta\beta}$ gives an indication of the accuracy of the beam tilt calibration. The errors of the other PCTF parameters are much less influenced by calibration errors. Their precise contribution can be deduced from eqs. (17a-17f) and (19), but is usually negligible compared to the contribution of the variances of the other coefficients needed for the calculation.

Experimental

Procedure

The procedure for measuring the PCTF parameters consists of the following steps:

a). Calibration of the microscope magnification and dark-field beam-tilt coils.

b). Recording of a set of images with induced beam tilts using the x and the y dark-field tilt coils.

c). Calculation of the cross correlation functions between the reference image (i.e. without induced beam tilt) and the images with induced tilts, followed by the determination of the displacement vectors from the maxima or (local) minima.

d). Fitting the measured displacements to a third-order (parallel) and a second order (perpendicular) polynomial.

Note that the alignment of the microscope is not a critical step, except the alignment of the pivot points which ensures that the beam remains focussed on the same area of the sample, independent of the beam tilt. Of course, the spherical aberration is dependent on the position of the specimen in the objective lens, and care must be taken to find a reproducible specimen height.

Table 2. Experimental conditions and calibration data for the three microscopes used.

microscope	CM12T	CM20UT	CM30ST
accelerating voltage (kV)	100	200	300
magnification (x 1000)	60	250	260
magn. calibration (nm/pix)	0.584	0.092	0.115
tilt calibration (mrad/step)	3.49	2.93	2.10
maximum induced tilt (mrad)	40	30	20

The experiments were performed on a Philips CM12-Twin microscope, a CM20-UltraTWIN microscope and a CM30-SuperTWIN microscope. Experimental details are summarized in Table 2. All instruments were equipped with an LaB_6 cathode. The Philips CM series of TEM are computer controllable by means of a serial port. The images were recorded with a Gatan 622 video camera with image intensifier. The TEMDIPS computer system (TVIPS GmbH) was used for on-line video-image processing and microscope control (via RCS remote control). The most important microscope control functions used were the direct control of the pre-specimen x- and y-deflection coils of the TEM to induce the dark field tilt angles. All the image processing and microscope control commands were executed by means of command procedures, without human intervention.

Calibrations

On the CM12, the calibrations were performed using separate specimens. For the calibration of the beam tilt coils, the relative shift of the {111} reflections of polycrystalline aluminium induced by a specified amount of beam tilt (in "ticks", the smallest unit-of-change) were measured. Reproducibility in controlling the x- and y-deflection coils was 0.7%. For the calibration of the magnification, a test specimen (2160 lines/mm) was used at M=6300 (0.5% measuring error). The calibration was extended to a magnification of 60,000 via independent calibrations on micrographs. The total error in this calibration was 0.5% measuring error + 1% error in magnification reproducibility.

On the CM20-UT, a specimen consisting of an oriented Au film on carbon foil was used for the calibration of both the magnification and the beam tilt coils. The magnification (nominally 250,000) was calibrated by taking lattice images and measuring the distance to the {200} spots in the computed diffractogram (measuring error 0.5%). The beam tilt coils were calibrated by measuring the beam tilt induced shifts of the {800} spots. The measuring error for this calibration was 0.35%.

On the CM30-ST, a specimen consisting of gold particles on a carbon film was used both for the calibrations and for the tilt-series, at a magnification of 260,000. The magnification was calibrated using the {111} Au spots in the computed diffractogram (measuring error 1 %). The beam tilt coils were calibrated by monitoring the {111} and {200} reflections in the dark-field mode (measuring error about 1 %). The advantage of using the same specimen for both calibrations and tilt series at one magnification is that no

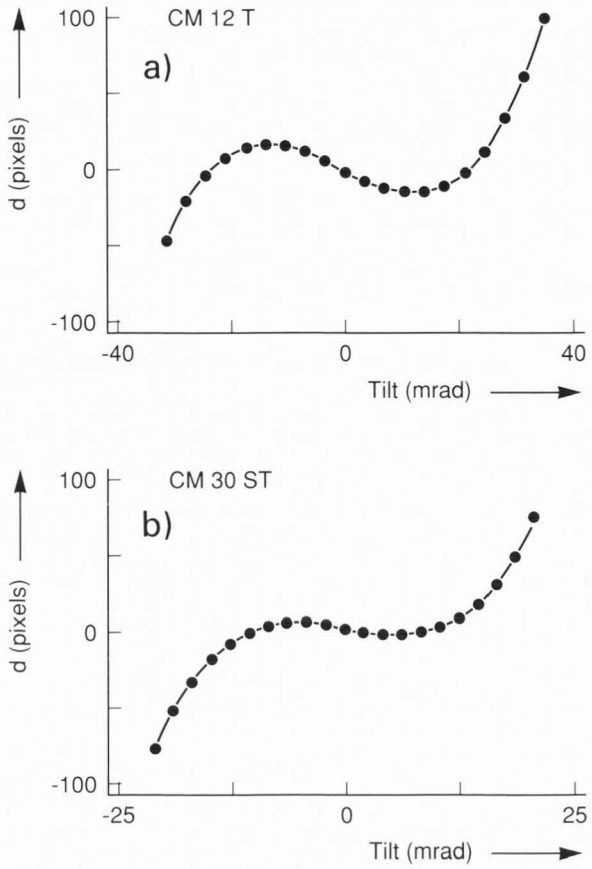

Fig. 5. Parallel image displacement as a function of induced beam tilt (mrad), for two cases. Top: the CM12-TWIN using the y tilt-coils, f = -500 nm. Bottom: the CM30-SuperTWIN using the x tilt-coils, f = -150 nm. The dots indicate the measured points, the drawn line is the fitted third-order polynomial.

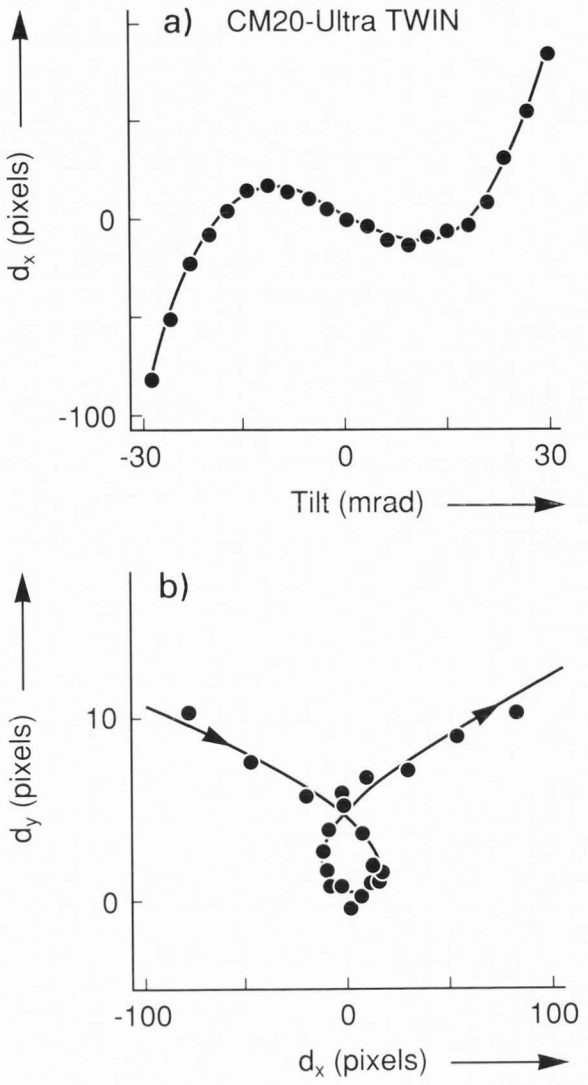

Fig. 6. Image displacement as a function of induced beam tilt as measured on the CM20-UltraTWIN microscope, using the x tilt-coils. The dots indicate the measured points, the drawn lines are simulated displacements using the fitted parameters (Table 4). Top: parallel displacement as a function of beam tilt. Bottom: trajectory of the image shift parallel (d_x) and perpendicular (d_y) to the induced tilt. Note the difference in scale along the vertical and horizontal axes.

additional errors are introduced. On the other hand, the magnification must be chosen low enough to enable the measurement of an appreciable image shift. Note that the test specimen used here is in fact not an ideal calibration specimen, as the lattice of the small Au particles may be slightly deformed, resulting in d_{hkl} values slightly different from those of bulk Au.

The calibrations are summarized in Table 2. The tilt calibrations are given as the incremental amount of tilt induced for each step of the tilt series.

Results

Determination of the spherical aberration constants

For the determination of the C_s, only one tilt series is necessary, using the parallel component of the displacement. Several tilt series were recorded on each microscope. The experiments on the CM12 were performed on a polycrystalline Au sample, those on the CM20 and CM30 were performed on a sample of Au particles on a carbon film. Figures 5 and 6 (top) give some examples of the measured (parallel) displacements as a function of beam tilt. The experimental measurements fit the theoretical third-order curve very well. Table 3 gives an overview of the estimated values of the C_s, together with their measuring errors which can be found from the covariance matrix of the (three) estimated coefficients. For the sake of clarity, we have given the values of C_s rather than C_4 which is found from eq. (17a), assuming an electron wavelength in accordance with the nominal accelerating voltage. As mentioned before, the wavelength is not a necessary parameter for the reconstruction of the PCTF (eq. (3)).

It is clear that for the measurement of the C_s a measuring error better than 1% can be reached in most cases. This is much better than the precision reported by Budinger and Glaeser (1976), or the precision obtained by Krivanek (1976) using the method of analysing the diffractograms of images of an amorphous specimen. (Recently, however, this method has been extended by Coene and Denteneer (1991), yielding

precisions in the measurement of C_s similar to ours.) However, errors in the calibration contribute significantly to the absolute error made in the determination. The error in C_4 caused by calibration errors is (from eqs. (19) and (17a)):

$$\frac{\Delta C_4}{C_4} = \sqrt{\left(\frac{\Delta M}{M}\right)^2 + \left(3\frac{\Delta r}{r}\right)^2}, \qquad (20)$$

where $\Delta M/M$ and $\Delta r/r$ are the errors in magnification calibration and beam tilt calibration, respectively. For the experiments on the CM12 we find a calibration error of 2.5%, for the CM20 1.2% and for the CM30 3.1%. Clearly, the error in the calibration of the beam tilt is (in most cases) the dominating factor for the accuracy (combined measuring and calibration errors) in the estimation of C_s. On the other hand, an indication of this error can be obtained by comparing the C_s values found from the x tilt series with those found from the y series, as the x and y beam tilts are calibrated separately. It is then found (see Table 3) that these differences are usually well below the error caused by the beam tilt calibration. Therefore these errors may have been overestimated, especially for the experiments performed on the CM20 and CM30 high-resolution microscopes. When the calibration is performed very carefully, an accuracy around 1.5% can be reached (CM20-UltraTWIN), including the variance in the fitted coefficient as well as the variance caused by calibration errors.

Determination of beam tilt, defocus and astigmatism

The determination of all six parameters of the PCTF requires the analysis of both the parallel and the perpendicular components of the displacements resulting from induced tilts in the x and y direction. The results of one experiment on the CM20 microscope are given in Table 4. The values of the beam tilt are given in mrads rather than $(nm)^{-1}$ and the defocus values f are given rather than λf which would be found from eq. (18). This is done for clarity, as pointed out in previous sections the wavelength is in fact just a scaling parameter between the conventionally used values and those actually needed in the PCTF. The parameters found were subsequently used to simulate the displacement trajectory as a function of the x beam tilt and compared to the experimental trajectory (Fig. 6, bottom). The fit is quite good, almost all the experimental points are within one pixel of the theoretical curve. The coefficients fitted from the perpendicular displacements are generally not very accurate, obviously because the measuring errors (one pixel) are large compared to the displacements (one to ten pixels). This causes the rather large inaccuracy in the determination of both the amount and the direction of the astigmatism. In addition, a small amount of sample drift (which influences mainly the first-order coefficients) has the same influence as an extra amount of astigmatism. In the experiments performed here, care was taken to assure a minimum amount of specimen drift, but even a drift of about 2 pixels during the recording of one tilt series should in fact be corrected for.

For the determination of the beam tilts and the defocus, the perpendicular displacements are not important. In Table 5, the average measuring errors and absolute accuracies are given with which these parameters have been measured for the three microscopes used. The measuring errors are derived from the covariance matrix of the fitted coefficients. To calculate the accuracy of the measurements, we have to consider the influence of the uncertainties of other parameters (C_4 is needed to calculate the beam tilt, C_4 and beam tilt are needed to calculate the defocus). In addition, the influence of the calibration errors is taken into account. Still, from Table 5, it is clear that the stochastic error of the relevant coefficient is the most important error source. Under HREM conditions (CM20 and CM30 experiments), it is possible to obtain an accuracy of 0.045 mrad in the determination of the beam tilt, and of 5 nm in the defocus. Note that the values mentioned here are the absolute accuracies and not the reproducibility of the measurements within one calibration set (which would only give an indication of the variance of the fitted coefficients, see Koster and de Ruyter, 1992).

Table 3. Measured values for the spherical aberration constant C_s of three microscopes, with the calibration errors and the measuring errors found from the fit.

microscope	H.T. (kV)	calibration error (%)	tilt-coil	C_s (mm)	ΔC_s (mm)
CM12-T	100	2.5	x	2.14	0.015
			y	2.10	0.008
CM20-UT	200	1.2	x	0.510	0.004
			y	0.508	0.005
CM30-ST	300	3.0	x	1.19	0.006
			y	1.18	0.012

Table 4. Measured values of the beam tilt, defocus and astigmatism for a typical experiment on the CM20 UT microscope, with their standard deviations.

parameter	value	standard deviation	units
m_x	0.14	0.03	mrad
m_y	-1.06	0.04	mrad
f	-177	3	nm
A	12	6	nm
ϕ_a	10	10	deg.

Discussion and Conclusion

The accuracies for beam tilt, defocus and astigmatism presented here are better than the reproducibilities (i.e. statistical variance of the coefficients) reported for autotuning methods (e.g. Koster and de Ruyter, 1992). This indicates that the method presented here can be used to assess not only the reproducibility but also the absolute accuracy of existing autotuning methods. For the measurement of the C_s, the method proposed here is accurate (measuring error below 1%, accuracy around 1.5%) and is much faster than existing methods.

If we compare the accuracies presented in the results section with the accuracies which are needed (section on required accuracy of the PCTF parameters), it is clear that the measurement of the beam tilt (misalignment) meets the demands: an accuracy better than 0.05 mrad. The accuracies which have been obtained so far for the C_s (1.5%), defocus (5 nm) and astigmatism (around 10 nm) are promising but not quite good enough. In order to enhance the accuracy, a few improvements can be made. So far we have measured the displacements only to one pixel accuracy. Using a least-squares fit to a parabola, it should be possible (Koster and de Ruyter, 1991) to detect maxima in the cross-correlation images to an accuracy of 0.2 pixel. When a slow-scan CCD camera is used, this could be even improved to accuracies below 0.1 pixel. Apart from a higher accuracy in the measurement of the displacements, also the magnification calibration and the beam tilt calibration could thus be improved considerably, which is

Table 5. Average measuring error (Δm and Δf) and absolute accuracy (acc.) of beam tilt and focus measurements obtained from several measurements on the three microscopes.

microscope	magnification (x1000)	beam tilt (mrad)		focus (nm)	
		Δm	acc.	Δf	acc.
CM12-T	60	0.035	0.045	10	25
CM20-UT	260	0.035	0.045	3	5
CM30-ST	250	0.030	0.045	3	4

especially important for the accuracy obtained in the measurement of the C_s. Furthermore, sample drift may be corrected for, either afterwards or by taking a sufficient number of reference images (i.e. without induced beam tilt) during the recording of the series. This can be expected to result in more accurate measurements of especially the astigmatism. Finally, improvements may be possible in the fitting procedure itself, e.g. by fitting the whole set of data, coming from induced tilts along x and y, as a whole.

The type of sample on which this measuring procedure may be applied is either an amplitude object at lower resolution, or a weak phase-object at high resolution. Problems may arise when the object is neither, as for most crystalline specimens at high resolution. In that case, the object wavefunction depends on the beam tilt and the imaging theory is non-linear, so that the effect of an induced beam tilt cannot be described as a simple displacement of the image. The measuring of the parameters of the PCTF may then be performed on an amorphous part (e.g. caused by sample preparation) near the area of interest. On the other hand, the experiments performed on the sample consisting of Au particles on a carbon film indicate that if only *part* of the object is crystalline, the measurements are quite reliable. It seems possible to automate this accurate PCTF measuring procedure to the extent that it becomes an easy operation on most samples (although relatively slow and not dose-efficient). Then it becomes feasible to incorporate this measurement into an HREM image reconstruction procedure, to be performed right after recording the hologram or the focal series and subsequently to be used in the final reconstruction step.

Acknowledgement

We are indebted to Dr. D. Typke and to Prof. W. Baumeister of the Max-Planck Institut for Biochemistry in Martinsried and to the National Centre for High Resolution Electron Microscopy of the Delft University of Technology for the provision of laboratory facilities. We also like to thank T. Denteneer for helpful discussions on the statistical analysis of the data. Part of this work was financed by the BRITE/EURAM project nr. 3322.

References

Baba N., Oho E. and Kanaya K. (1987). An algorithm for on-line digital image processing for assisting automatic focussing and astigmatism correction in electron microscopy, *Scanning Microscopy* 1 1507-1514.

Budinger T.F. and Glaeser R.M. (1976). Measurement of focus and spherical aberration of an electron microscope objective lens, *Ultramicroscopy* 2 31-41.

Coene W.M.J. and Denteneer T.J.J. (1991). Improved determination of the spherical aberration coefficient in high resolution electron microscopy from micrographs of an amorphous object, *Ultramicroscopy* 38 225-233.

de Ruyter W.J., Rez P. and Smith D.J. (1990). Recent progress and plans in computer-controlled high resolution electron microscopy, *Proc. 12th ICEM (San Francisco Press, Inc.)* 1 154-155.

Erasmus S.J. and Smith K.C.A. (1982). An automatic focussing and astigmatism correction system for the SEM and the CTEM, *J. Microscopy* 127 185-199.

Frank J. (1973). The envelope of electron microscopy transfer functions for partially coherent illumination, *Optik* 38 519-536.

Kirkland E.J. (1984). Improved high resolution image processing of bright field electron micrographs, *Ultramicroscopy* 15 151-172.

Kirkland E.J. and Siegel B.M. (1979). Error sensitivity as a limit to resolution in computer image processing of electron micrographs *Optik* 53 181-196.

Koster A.J., van den Bos A. and van der Mast K.D. (1987). An autofocus method for a TEM, *Ultramicroscopy* 21 209-222.

Koster A.J. (1988). Signal processing for autotuning by beam tilt induced image displacement, *Scanning Microscopy Suppl.* 2 83-92.

Koster A.J. and de Jong A.F. (1991). Measurement of the spherical aberration coefficient of transmission electron microscopes by beam-tilt induced image displacements, *Ultramicroscopy* 38 235-240.

Koster A.J., de Ruyter W.J., van den Bos A. and van der Mast K.D. (1989). Autotuning with minimum electron dose, *Ultramicroscopy* 27 251-272.

Koster A.J. and de Ruyter W.J. (1992). Practical autoalignment of transmission electron microscopes, *Ultramicroscopy* 40 89-108.

Krivanek O.L. (1976). A method for determining the coefficient of spherical aberration from a single electron micrograph,*Optik* 45 97-101.

LePoole J.B. (1947). A new electron microscope with continuously variable magnification, *Philips Tech. Rev.* 2 33.

Lichte H. (1986). Electron holography approaching atomic resolution, *Ultramicroscopy* 20 293-304.

Lichte H. (1991a). Electron Image Plane Off-axis Holography of Atomic Structures, *Adv. Opt. Electr. Micr.* 12 25-91.

Lichte H. (1991b). Optimum focus for taking electron holograms, *Ultramicroscopy* 38 13-22.

Saxton W.O, Smith D.J. and Erasmus S.J (1983). Procedures for focussing, stigmating and alignment in high-resolution electron microscopy, *J. Microscopy* 130 187-201.

Smith D.J., Saxton W.O, O'Keefe M.A., Wood G.J. and Stobbs W.M. (1983). The importance of beam alignment and crystal tilt in high-resolution electron microscopy, *Ultramicroscopy* 11 263-282.

Van Dyck D. (1991). Future prospects for structure determination using HREM, *Proc. 49th EMSA (San Fransisco Press, Inc.)* 654-655.

Van Dyck D. and Op de Beeck M. (1990) New direct methods for phase and structure retrieval in HREM, *Proc. 12th ICEM (San Francisco Press, Inc.)* 1 26-27.

Wade R.H. and Frank J. (1977). Electron microscope transfer functions for partially coherent axial illumination and chromatic defocus spread, *Optik* 49 81-89.

Zemlin F., Weiss K., Schiske P., Kunath W. and Herrmann K.H. (1978). Coma-free alignment of high-resolution electron microscopes with the aid of optical diffractograms, *Ultramicroscopy* 3 49-60.

Editor's Note: All of the reviewer's concerns were appropriately addressed by text changes, hence there is no Discussion with Reviewers.